16th World Conference on Earthquake, 16WCEE 2017

Santiago Chile, January 9th to 13th 2017

Paper N° 1036

Registration Code: S-V1464579433

FINITE ELEMENT ANALYSIS OF CONCRETE SLAB-COLUMN CONNECTIONS SUBJECTED TO CYCLIC LATERAL LOADINGS

A.S. Genikomsou(1), M.A. Polak(2)

(1) Department of Civil and Environmental Engineering, University of Waterloo, Waterloo, Canada, Ph.D. student, agenikom@uwaterloo.ca

(2) Department of Civil and Environmental Engineering, University of Waterloo, Waterloo, Canada, Professor, polak@uwaterloo.ca

Abstract

Punching shear failure of reinforced concrete slabs can occur by additional shear stresses that are caused by lateral loads due to earthquakes that induce unbalanced moments to the slab-column connection. 3D nonlinear finite element analysis (FEA) of two interior reinforced concrete slab-column connections previously tested under constant gravity loads and pseudo-seismic loads are presented. Seismic loads are simulated by reversed cyclic horizontal displacements with increasing intensity. The two slabs differ in the value of the constant gravity load and this is examined in terms of their failure mode. Both specimens are analyzed using the damaged plasticity model for concrete offered in the ABAQUS software. In this plasticity damaged based model, damage can be introduced separate in tension and compression simulating the stiffness recovery of concrete after cracking, specifically, when cyclic loading takes place. The numerical analysis results are compared to the test results in terms of moment resistance and crack patterns. Both FEA and experimental results are in good agreement indicating the effectiveness of the finite element model. Finite element analysis can give an insight into the failure mechanisms and crack developments of concrete slabs; creating a basis for future parametric studies on many aspects in punching shear of reinforced concrete slabs located in seismic zones.

Keywords: finite element analysis; cyclic loading; concrete slabs; punching shear

1. Introduction

Punching shear failure can happen in reinforced concrete flat slabs due to the development of high shear stresses in the slab-column connection area. These shear forces are developed from gravity loads and/or by unbalanced moments and/or by movement during events such as earthquakes and high winds. A 3D state of stresses and strains is caused, resulting in principal tension stresses to be inclined with respect to the slab's plane. Cracks occur inside the slab into the vicinity of the column and then they propagate through the thickness of the slab to the bottom of the slab. These inclined cracks are developed around the column and consequently the column separates from the slab leading to punching shear failure. In modern research, 3D nonlinear FEA can be considered as an advanced numerical tool to analyze reinforced concrete slabs and give an insight into the slabs' behavior by predicting the possible failure modes, supporting the experimental conclusions and finally extending these conclusions where the test measurements are not known. Many researchers have conducted FEA of reinforced concrete slabs using the ABAQUS software [1] with the most recent research done by Genikomsou and Polak [2].

In this paper, two interior reinforced concrete slab-column connections without shear reinforcement previously tested [3] under vertical loading and reversed horizontal displacements are analyzed using ABAQUS [1] with the concrete damaged plasticity model. The previously calibrated concrete model is now considered with damage. A detailed description of all plasticity and damage parameters is presented. All the numerical results are compared to the test results in terms of load-deflection responses and crack patterns.

2. Test specimens

Two interior slab-column connections (SW1, SW5) that were previously tested by Bu and Polak [3] under gravity static and lateral cyclic loadings are analyzed. In the experiment, the slabs were tested "upside down" compared to the real slab-column system. These slabs were loaded in two stages during the test. At the beginning of the experiment, a vertical load that simulates the gravity loading was applied through the top column with a loading rate of 20 kN/min. The maximum vertical loads for the slabs SW1 and SW5 were 110 kN and 160 kN, respectively. Then, these vertical loads were kept constant and two horizontal actuators started to apply horizontal drift to the top and bottom columns at a distance 565 mm from the slab's faces following a specific loading path (Fig. 1). At a specific drift ratio each cycle was repeated three times. After the 0.75% of drift ratio, a cycle of 0.5% drift ratio was used between each group of three cycles of the same drift ratio. After the 3% of drift ratio the loading path was applied in increasing way without repeating each cycle. The gravity shear ratio V/V_n for the slab SW1 was 0.54 and for the slab SW5 was 0.68, where $V_n = 0.33\sqrt{f_c^{'}}b_o d$ (MPa), b_o denotes the perimeter length of the critical section and d is the effective thickness of the slabs equal to 90 mm. The dimensions of both slabs are in plan 1800x1800 mm with simple supports located at 1500x1500 mm. The thickness of both slabs was 120 mm and the cross section area of the columns was 200x200 mm. Both top and bottom column stubs were extending from the top and bottom surfaces 700 mm. Fig. 2 shows the dimensions and loading of the slabs, while Table 1 presents the material properties of the slabs. The flexural reinforcement ratio of the bottom (tension) side of the slabs is 1.05% (10M at 100 mm) for the outer bars and 1.3% (10M at 90 mm) for the inner bars to obtain the same moment capacities in both orthogonal directions. On the compression face of the slabs (top surface) the flexural reinforcement ratio is 0.58% for both directions (10M at 200 mm).

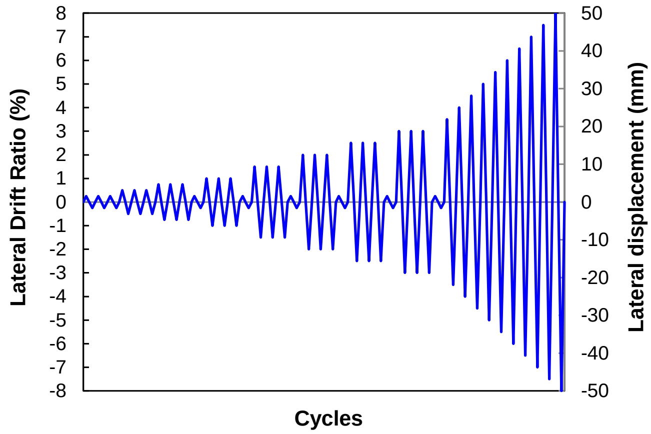

Fig. 1 – Loading path.

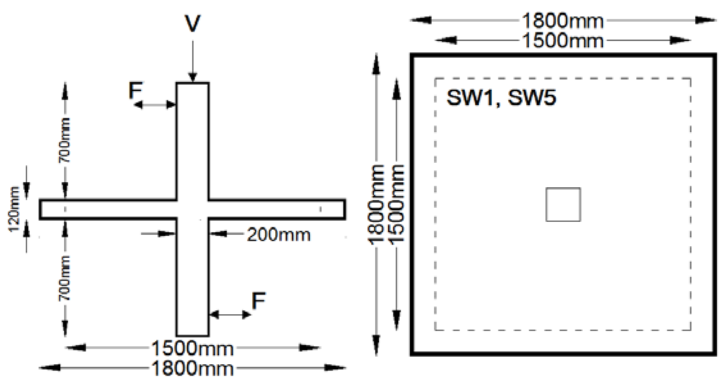

Fig. 2 – Loading path.

Table 1 – Material properties of the tested slabs

	Concrete		**Reinforcement**			
Slab specimen	**f'_c (MPa)**	**f'_t (MPa)**	**f_y (MPa)**	**ε_y (mm/mm)**	**f_t (MPa)**	**ε_t (mm/mm)**
SW1	35	2.9	470	0.0024	650	0.2
SW5	46	3.1				

Both specimens failed in punching shear during the experiments. Fig. 3 shows the horizontal load versus lateral drift ratio curves for both slabs. The peak lateral load of the slab SW1 was 56 kN at drift ratio of 2.8%, while the peak lateral load of the slab SW5 was 60 kN at drift ratio 2.6%. All cracks on the slabs started to develop from the corners of the columns on the tension (bottom) surface, when the gravity loads were applied. The cracking propagated to all edges and corners of the slabs. On the top (compression) surface of the slabs, the first cracks were found at approximately 0.6 to 0.75% drift ratio. These first cracks developed from the corners in the direction perpendicular to the lateral loading direction. Fig. 4 shows the crack pattern of the slab SW1 at failure, while Fig. 5 shows the failure cracking of the slab SW5.

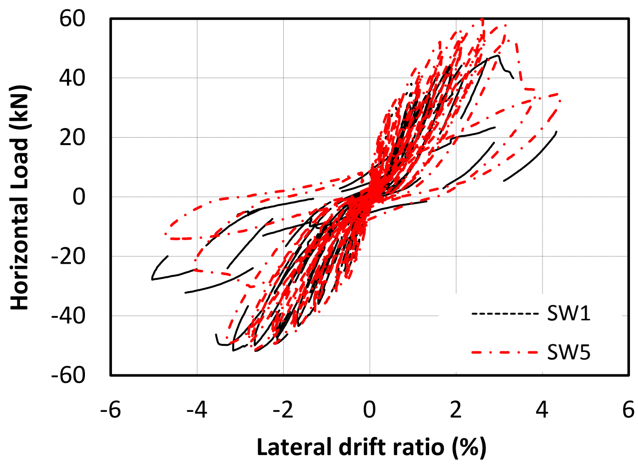

Fig. 3 – Horizontal load versus drift ratio (test results).

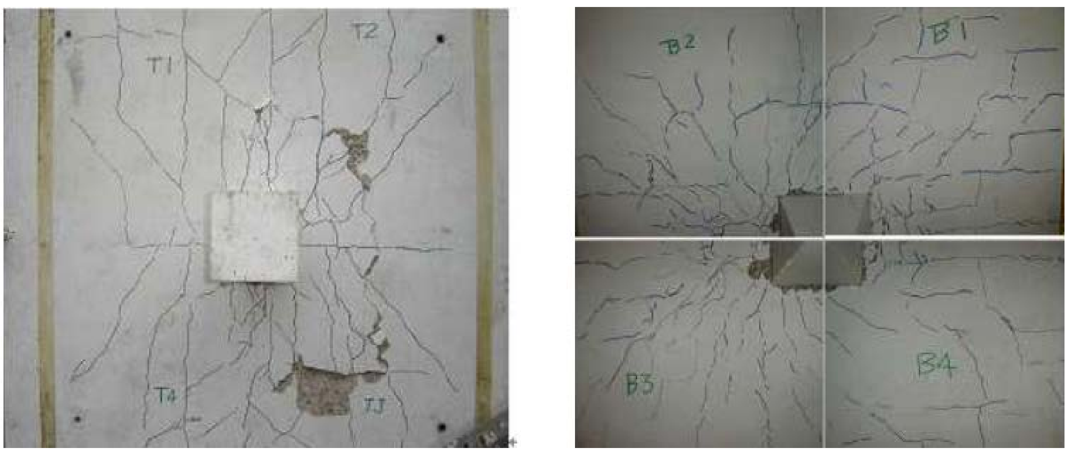

Fig. 4 – Crack patterns at failure at top (left) and bottom (right) surfaces of the slab SW1 [3].

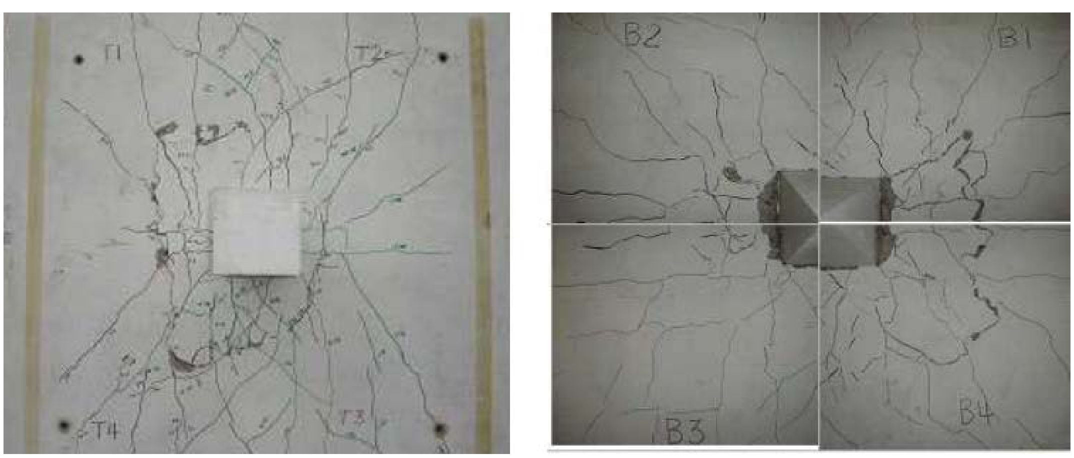

Fig. 5 – Crack patterns at failure at top (left) and bottom (right) surfaces of the slab SW5 [3].

3. Finite Element Simulations

3.1 Concrete Damaged Plasticity model

The concrete damaged plasticity model considers both the tensile cracking and compressive crushing of concrete as possible failure modes [4]. The yield function of the concrete damaged plasticity model considers the effective stress space, where the effective stress is defined as: $\overline{\sigma} = \sigma/(1-d) = E_o(\varepsilon - \tilde{\varepsilon}^{pl})$, where E_o denotes the initial modulus of elasticity, $\tilde{\varepsilon}^{pl}$ is the equivalent plastic strain and d is the damage variable that denotes the stiffness degradation. The plastic potential function that is employed in the model is a non-associated Drucker-Prager hyperbolic function. According to ABAQUS manual [1], cracking initiates at points where the maximum principal strains are positive. The direction of cracking is viewed in the Visualization module of ABAQUS/CAE; the direction of the vector normal to the crack plane is assumed parallel to the direction of the maximum principal plastic strains. Concrete in tension can be characterized by a stress-crack displacement response instead of a stress-strain relationship due to its brittle behavior. Different types of stress-crack displacement curves (linear, bilinear or exponential) that describe the tension softening response of concrete can be considered. In this research, the bilinear tension softening relationship is adopted. Fig. 6 illustrates the tensile stress-strain curve for the specimen SW1 based on the fracture energy (G_f) cracking criterion. Fracture energy is calculated using the CEP-FIP Model Code 1990 [5]. Concrete in compression is modelled with the Hognestad parabola. Fig. 7 shows the compressive stress-strain relationship of the slab SW1, where, both the compressive stress-inelastic strain relationship and the compressive stress-plastic strain relationship are shown. In ABAQUS, the uniaxial stress-inelastic strain curve is converted automatically into stress versus plastic strain. Plastic strain considers the damage parameters by showing stiffness degradation during the unloading, while inelastic strain considers the same stiffness as the initial. Table 2 shows the compressive and tensile damage parameters with the strains for the slab SW1. Stiffness recovery through the specification of the stiffness recovery factors (wt and wc) can be considered in the concrete damage plasticity model especially when concrete is tested under cyclic loading (Fig. 8). All other needed model parameters of the concrete damaged plasticity model, such as the dilation angle, are taken from a previous research [2].

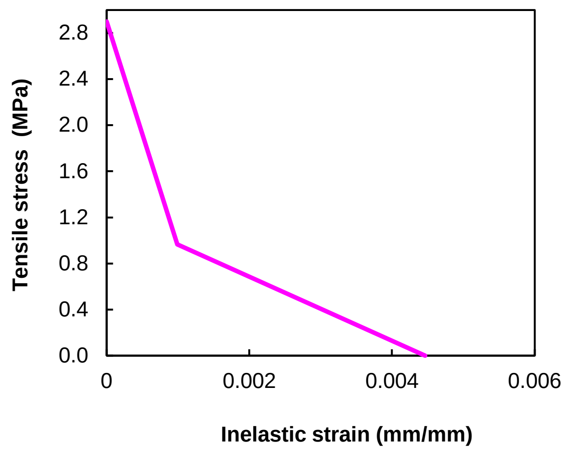

Fig. 6 – Tensile stress-strain curve for the slab SW1.

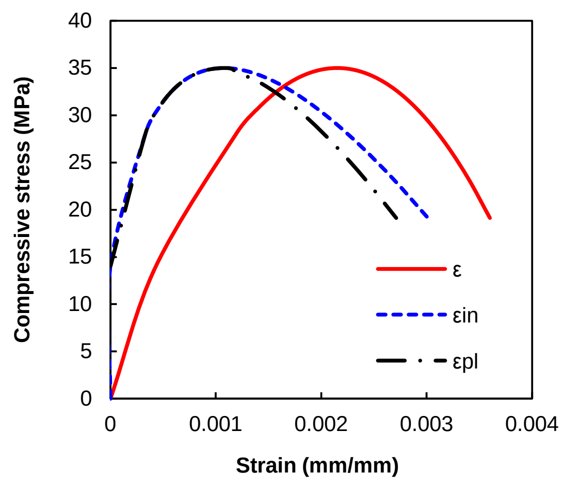

Fig. 7 – Compressive stress-strain curves for the slab SW1.

Table 2 – Compressive (dc) and tensile (dt) damage parameters for the slab SW1.

Compressive strain	dc	Tensile strain	dt
0	0	0	0
0.0004	0	0.0010	0.6007
0.0012	0	0.0045	0.9000
0.0014	0		
0.0016	0		
0.0018	0		
0.0020	0		
0.0022	0		
0.0024	0.1120		
0.0026	0.1325		
0.0028	0.1571		
0.0030	0.1872		
0.0032	0.2249		
0.0034	0.2736		
0.0036	0.3388		

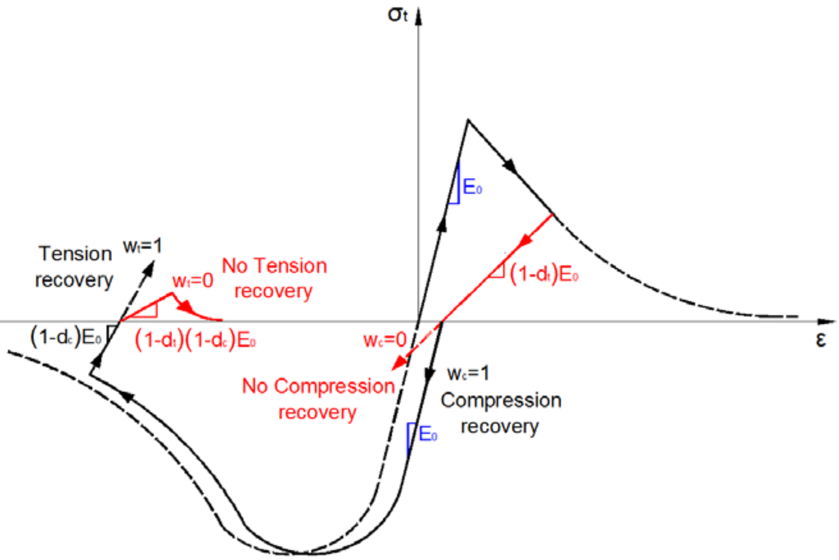

Fig. 8 – Uniaxial load cycle (tension-compression-tension) assuming default values for the stiffness recovery factors.

3.2 FEA methodology

Half of the real slab-column connections are modelled in ABAQUS due to symmetry. Three-dimensional continuum hexahedral (brick) elements are considered for modeling the concrete slabs. These elements are linear (8-noded) and they use reduced integration (C3D8R). The flexural reinforcement is modelled with three-dimensional linear (2-noded) truss elements, named in ABAQUS as T3D2. No bond-slip behavior between concrete and reinforcement is considered and the embedded method is chosen that assumes perfect bond between concrete and reinforcement. However, the interaction between concrete and reinforcement is indirectly considered through the concrete material modeling by using tension stiffening for the tensile behavior. The mesh size is considered equal to 20 mm based on a previous research [2]. Simple supports that resist vertical movement are introduced along the bottom edges of the slabs and at the top edges of the slabs normal to the horizontal loads. In the first step, static analysis is conducted where the gravity load is applied that simulates the vertical load that was applied to the column during the tests. At the second step, the gravity loads continues to be applied as constant, while a dynamic implicit analysis under displacement control is conducted in order to simulate the applied horizontal displacements. In the numerical simulations monotonic analysis is conducted for both slab-column connections.

4. Finite Element Analysis results

4.1 Load-deflection responses and drift ductility

Fig. 9 shows the backbone curves of the load-drift ratio responses of the specimens SW1 and SW5, respectively, where the FEA results are compared to the test results. The numerical results show similar response for both slabs compared to the test results. In the present analyses viscoplastic regularization (viscosity parameter=0.00001) and damage parameters in both tension and compression are considered in the concrete damaged plasticity model. Both slabs failed in punching shear after attaining the maximum lateral load. Specimen SW5 had higher gravity load and failed at a higher lateral load (61 kN) compared to the slab SW1 that failed at a load of 53 kN.

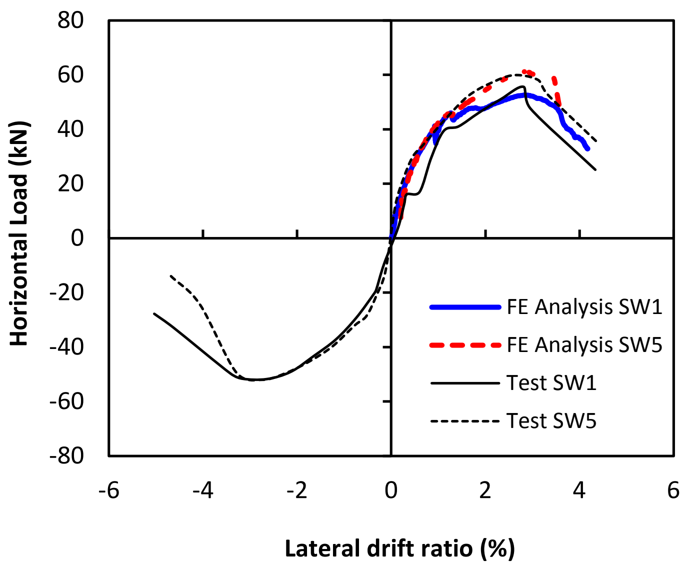

Fig. 9 – Backbone curves of the load-drift ratio responses.

Table 3 – Peak lateral load and drift ductility

		Test results			FEA results		
Slab specimen	**V/Vn**	**Peak lateral load (kN)**	**Drift ratio (%)**	**Drift ductility at peak load (%) [6]**	**Peak lateral load (kN)**	**Drift ratio (%)**	**Drift ductility at peak load (%) [6]**
SW1	0.54	56	2.8	1.78	53	2.8	2.60
SW5	0.68	60	2.6	1.81	61	2.8	2.00

The displacement ductility is calculated as the ratio of the certain displacement to the yield displacement ($\mu = D/D_y$). The method proposed by Pan and Moehle (1989) [6] is considered in this paper, where the yield displacement is calculated using the backbone curves. The line starts from the origin and connects the points

$(2/3)P_{\max}$ and $P_{\max}$ defines the yield displacement (D_y). Table 3 shows the drift ductility at the peak load for both slabs based on the test and FEA results. The drift ratio at the first yield according to the test results using the method proposed by Pan and Moehle [6] is equal to 1.58% and 1.44% for the slab SW1 and SW5, respectively. Using the same method in FEA the drift ratio at the first yield is equal to 0.72% and 0.93% for the slab SW1 and SW5, respectively. Based on the experimental findings the drift ratio at the first yield of the flexural reinforcement is equal to 1.33% and 1.04% for the slab SW1 and SW5, respectively. This indicates that during the tests the yielding of the flexural reinforcement happened prior to punching shear failure. However, this yielding for both slabs was not significant and thus the slabs failed due to punching shear.

4.2 Crack patterns

Cracking in the numerical analyses started on the bottom tension surfaces of the slabs. These cracks appeared first at the corners of the columns when the vertical loading applied and then they propagated toward all four edges and corners. On the top compressive surfaces the initial cracks observed at approximately 0.7% drift ratio and started to propagate from the corners of the columns perpendicular to the lateral loading direction. Fig. 10 and 11 show the FEA crack development of slabs SW1 and SW5, respectively, where a side view of the slabs is presented showing the internal cracking at the connection at failure.

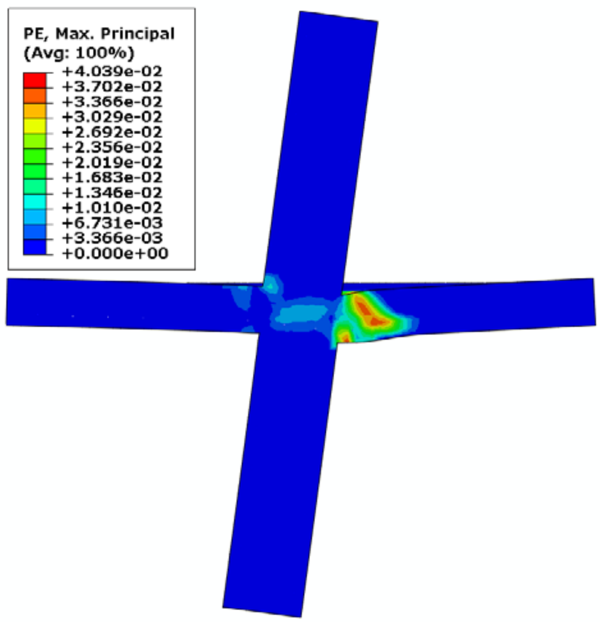

Fig. 10 – FEA crack pattern of specimen SW1. Contour plot of the maximum principal plastic strains at peak load.

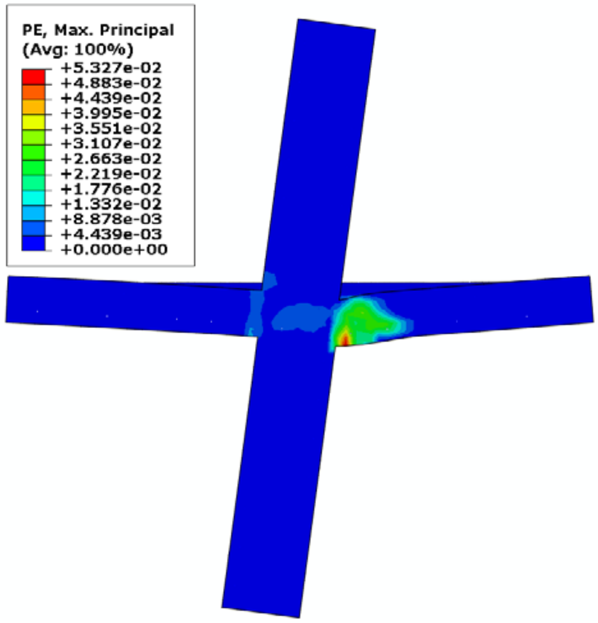

Fig. 11 – FEA crack pattern of specimen SW5. Contour plot of the maximum principal plastic strains at peak load.

5. Conclusions

Finite element analyses of two interior reinforced concrete slabs previously tested under cyclic loading are considered. The slabs are analyzed in ABAQUS in terms of ultimate load, ultimate displacement and cracking propagation by performing pushover analysis. The concrete damaged plasticity model with proper damage and stiffness recovery parameters predicts accurately the punching shear response of the slabs. Future studies will consider the whole cyclic analysis for both slabs, where the stiffness recovery and damage parameters will be further examined in order to simulate the pinching effect that was appeared in the experimental findings. The finite element analysis results confirm the ability of the proposed model for predicting the punching shear failure in concrete slabs. Test and analytical results showed a punching shear failure for both slabs. Future investigation will consider slab-column connections with punching shear reinforcement.

6. Acknowledgements

The authors are grateful for the financial supported provided by a Grant from the Natural Sciences and Engineering Research Council (NSERC).

7. References

[1] ABAQUS Analysis user's manual 6.12-3 2012. Dassault Systems Simulia Corp, Providence, RI, USA

[2] Genikomsou AS, Polak MA (2015): Finite element analysis of punching shear of concrete slabs using damaged plasticity model in ABAQUS. *Engineering Structures*, **98**(4), 38-48.

[3] Bu W, Polak MA (2009): Seismic Retrofit of Reinforced Concrete Slab - Column Connections using Shear Bolts. *ACI Structural Journal*, **106**(4), 514-522.

[4] Lee J, Fenves GL (1998): Plastic-damage model for cyclic loading of concrete structures. *ASCE Journal of Engineering Mechanics*, **124**(8), 892-900.

[5] Comité Euro-International du Béton, CEB-FIP-model Code 1990: Design code, Thomas Telford, London, 1993.

[6] Pan A, Moehle JP (1989): Lateral Displacement Ductility of Reinforced Concrete Flat Plates. *ACI Structural Journal*, **86**(3), 250-258.